VII. Lyα (and other lines)

A. Motivations

- Strongest transition of HI
- Major coolant of HII regions
- Only diagnostic for much of the Universe
- We will explore Lyα and other line transitions

B. Physics

- Energies (n levels)

$$E_n = -\frac{1}{2}\mu c^2 \frac{(Z\alpha)^2}{n^2} \tag{1}$$

  - μ: Reduced mass
  - $\mu \approx 0.999 m_e$ for H, closer to m_e for higher Z
  - Hydrogen
    - Ground State: $E_1 = -13.6$ eV
    - 1st Excited State: $E_2 = -3.4$ eV

Lyman Series

Transition	n	$E_n - E_1$ (eV)	λ_{rest} (Å)	λ_{exp} (Å)
Lyα	2	10.200000	1215.6845	1215.6701
Lyβ	3	12.088889	1025.7338	1025.7223
Lyγ	4	12.750000	972.54759	972.5368
Lyδ	5	13.056000	949.75351	949.7431
Lyϵ	6	13.222223	937.81375	937.8035
Ly6	7	13.322449	930.75844	930.7483
Ly7	8	13.387500	926.23580	926.2257
Ly8	9	13.432099	923.16041	923.1504
Ly9	10	13.464000	920.97310	920.9631
Ly10	11	13.487604	919.36139	919.3514
Ly11	12	13.505556	918.13933	918.1294
Ly12	13	13.519527	917.19053	917.1806
Ly13	14	13.530613	916.43908	916.429
Ly14	15	13.539556	915.83374	915.824
Ly15	16	13.546875	915.33891	915.329
Ly16	17	13.552942	914.92921	914.919
Ly17	18	13.558025	914.58616	914.576
Ly18	19	13.562327	914.29604	914.286
Ly19	20	13.566000	914.04849	914.039
Ly∞	∞	13.6	912.6	

▲ Difference between λ_{rest} and λ_{exp} is mainly due to spin-orbit coupling (coming soon)

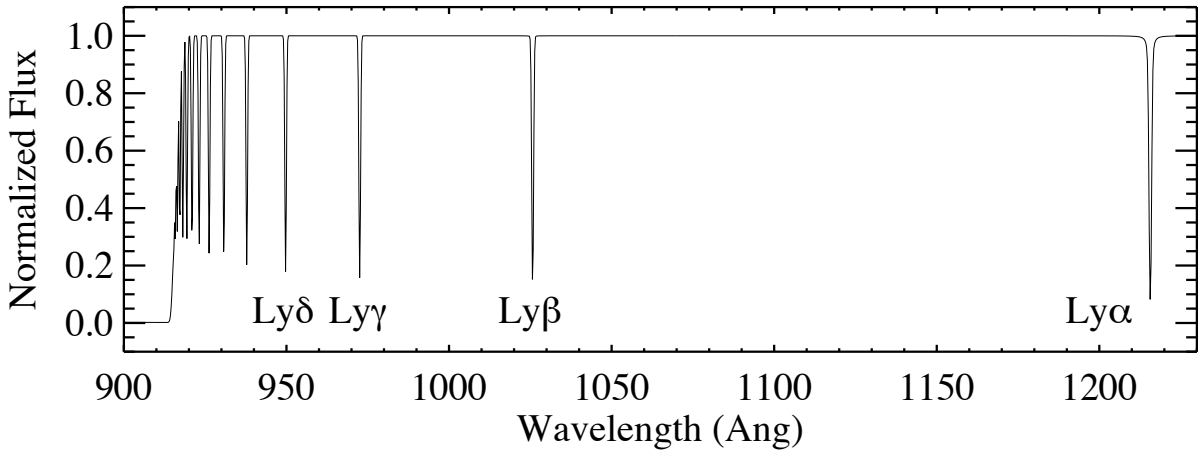

- Spin-Orbit Coupling
  - ◇ Classical motivation
    - ▲ e^- rest frame → Observes a magnetic field due to the current driven by the nucleus

$$\vec{B} = -\frac{1}{c}\vec{v} \times \vec{E} = \frac{1}{m_e c r}\, \vec{\ell}\, \frac{d\phi}{dr}$$

    - ▲ ϕ is the electrostatic potential
    - ▲ Energy

$$E = -\vec{\mu}_s \cdot \vec{B} \qquad \text{with} \quad \vec{\mu}_s = -\frac{eg\vec{s}}{2m_e c}$$

      - ○ $g \approx 2$ for an electron
      - ○ This energy is $2\times$ the relativsitic (correct) value
      - ○ Our 'classical' treatment failed to properly account for the transformations between non-interial frames
  - ◇ Proper Hamiltonian

$$H_{SO} = \frac{1}{2m_e^2 c^2}\, \vec{s} \cdot \vec{\ell}\, \frac{1}{r}\, \frac{d\phi}{dr} \tag{2}$$

  - ◇ Degenerate Perturbation theory
    - ▲ Our unperturbed states $|n\ell m m_s>$ (ignoring R-S Coupling) are highly degenerate
    - ▲ Brute force: Find the linear combination of $|n\ell m m_s>$ which diaganolize $H_{SO} \equiv V^{(1)}$
    - ▲ Shortcut: Identify an operator which commutes with $H^{(0)}$ and H_{SO} and uniquely identifies the degenerate states → $\vec{J}$

$$\vec{L}\cdot\vec{S} = \frac{1}{2}\left(|\vec{J}|^2 - |\vec{L}|^2 - |\vec{S}|^2\right)$$

◇ Energies

$$E_{SO} = < H_{SO} > = \frac{1}{2}C\,[\,j(j+1) - \ell(\ell+1) - s(s+1)\,] \tag{3}$$

▲ C is a constant

▲ For fixed $\vec{L}$ and $\vec{S}$,

$$\Delta E_{SO} = E_{J+1} - E_J = C(j+1)$$

◇ Example: Hydrogenic ion

▲ $\phi = Ze^2/r \;\Rightarrow\; d\phi/dr = -Ze^2/r^2$

$$H_{SO} = \frac{Ze^2}{2m_e^2c^2}\frac{1}{r^3}\vec{L}\cdot\vec{S}$$

▲ Perturbation theory

$$\begin{aligned} < H_{SO} > &= <nj'm'\ell's'|H_{SO}|njm\ell s> \\ &= \frac{Ze^2}{2m^2c^2}\Big\langle\frac{1}{r^3}\Big\rangle_{n\ell\ell'} <nj'm'\ell's'|\frac{1}{2}(J^2 - L^2 - S^2)|njm\ell s> \\ &= \frac{Ze^2}{2m^2c^2}\frac{\hbar^2}{2}\Big\langle\frac{1}{r^3}\Big\rangle_{n\ell}\;[\,j(j+1) - \ell(\ell+1) - s(s+1)\,]\,\delta_{j'j}\delta_{m'm}\delta_{\ell'\ell}\delta_{s's} \end{aligned}$$

▲ As expected, $< H_{SO} >$ is diagonal

▲ For explicit calculation

$$\left\langle\frac{1}{r^3}\right\rangle_{n\ell} = \frac{Z^3}{a_0^3}\frac{1}{n^3\ell(\ell+\frac{1}{2})(\ell+1)} \tag{4}$$

▲ Hydrogen 2p level (Z=1; n=2; $\ell = 0, 1; j = 1/2, 3/2$)

$$< H_{SO} >= \begin{cases} 0 & 2^2\mathrm{S}_{\frac{1}{2}} & (\ell = 0) \\ \frac{mc^2\alpha^4}{96} & 2^2\mathrm{P}_{3/2} & (\ell = 1; j = 3/2) \\ \frac{-mc^2\alpha^4}{48} & 2^2\mathrm{P}_{1/2} & (\ell = 1; j = 1/2) \end{cases}$$

▲ $2\mathrm{P}_{3/2}$ - $2\mathrm{P}_{1/2}$ splitting $= 4.5 \times 10^{-5}$ eV ≈ 1 km/s

▲ Note, relativisitic effects are of order α^4 and <u>cannot</u> be ignored!!

◇ One can also invert the problem to examine α

▲ Measure $< H_{SO} >$ in the lab

▲ Measure $< H_{SO} >$ at $z = 2$

▲ If there is a change, α is varying!

- Relativistic Correction

◇ Non-relativistic: K.E. $= p^2/2m$

◇ Expanding to the next term in v^2/c^2 from the Lagrangian

$$\text{K.E.} = \frac{p^2}{2m}\left(1 - \frac{1}{4}\frac{v^2}{c^2}\right) \tag{5}$$

◇ Relativstic perturbation: $H = H^{(0)} + H_{rel}$

$$H_{rel} = -\frac{1}{2mc^2}\left(\frac{p^2}{2m}\right)^2 \tag{6}$$

▲ No spin dependence, spherically symmetric

▲ $[H_{rel}, L^2] = [H_{rel}, L] = 0$

▲ Standard $|n\ell m m_s>$ diagonalize H_{rel}

◇ Trick

$$H_{rel} = -\frac{1}{2mc^2}\left(H^{(0)} - V^{(0)}\right)^2$$

◇ Computing the energies

$$< H_{rel} > = -\frac{1}{2mc^2}\left[(E_n^{(0)})^2 + 2E_n^{(0)}Ze^2\left\langle\frac{1}{r}\right\rangle_{n\ell} + Z^2e^4\left\langle\frac{1}{r^2}\right\rangle_{n\ell}\right] \tag{7}$$

$$= \frac{-Z^4\alpha^4mc^2}{2n^3}\left(\frac{1}{\ell + \frac{1}{2}} - \frac{3}{4n}\right) \tag{8}$$

◇ Combine with spin-orbit

$$< H_{SO} > + < H_{rel} >= \frac{-Z^4\alpha^4mc^2}{2n^3}\left[\frac{1}{j + \frac{1}{2}} - \frac{3}{4n}\right] \tag{9}$$

▲ No explicit ℓ dependence!

▲ Higher $j \Rightarrow$ Higher energy (3rd Hund's rule)

◇ Example: Hydrogen

$$\Delta E = -7.25 \times 10^{-4}\text{eV}\ \frac{1}{n^3}\left[\frac{1}{j + \frac{1}{2}} - \frac{3}{4n}\right]$$

State	n	j	$< H_{SO} > + < H_{rel} >$
$1\,^2\text{S}_{\frac{1}{2}}$	1	$\frac{1}{2}$	-1.8×10^{-4} eV
$2\,^2\text{S}_{\frac{1}{2}}$, $2\,^2\text{P}_{\frac{1}{2}}$	2	$\frac{1}{2}$	-5.7×10^{-5} eV
$2\,^2\text{P}_{\frac{3}{2}}$	2	$\frac{3}{2}$	-1.1×10^{-5} eV

▲ Does this explain our difference between λ_{theory} and λ_{exp} from before?

▲ Wavelength shift

$$\frac{\Delta\lambda}{\lambda} = -\frac{\Delta E}{E}$$

▲ Calculating ΔE from the above table and accounting for the relative degeneracy of the $2\,^2\mathrm{P}_{\frac{1}{2}}$, $2\,^2\mathrm{P}_{\frac{3}{2}}$ states

$$\begin{aligned}\Delta E &= \frac{1}{3}\left[\, 2\Delta E_{1S\rightarrow 2P_{\frac{3}{2}}} + \Delta E_{1S\rightarrow 2P_{\frac{1}{2}}} \,\right] \\ &= 1.55 \times 10^{-4}\ \mathrm{eV}\end{aligned}$$

▲ Therefore

$$\Delta\lambda = \frac{\Delta E}{E} \times 1215.68\text{Å} = -0.0138\text{Å}$$

▲ Success!

- Spontaneous emission coefficient
  - ◇ Identical for each transition
  - ◇ A value

$$A_{\mathrm{Ly}\alpha} = A_{21} = 6.265 \times 10^8\ \mathrm{s}^{-1} \tag{10}$$

C. Line Profile (valid for any line)

- Express the opacity

$$\kappa_\nu = n_j s_{jk}(\nu) \tag{11}$$

  - ◇ n_j = density of species in state j
  - ◇ s_ν = photon cross-section at frequency ν for a transition to state k
- Define the line profile: ϕ_ν

$$s_\nu = s_{jk}\phi_\nu \tag{12}$$

  - ◇ $s_{jk} = \int_0^\infty s_\nu\, d\nu$
  - ◇ $\phi_\nu\, d\nu$ is the probability an atom can absorb a photon in $\nu, \nu + d\nu$
- Naive guess: Delta function
  - ◇ Assume all of the particles are at rest
  - ◇ Assume the transition can only occur at $\nu = \nu_{jk}$
  - ◇ This amounts to:

$$\phi_\nu = \delta\left(\, \nu - \nu_{jk} \,\right) \tag{13}$$

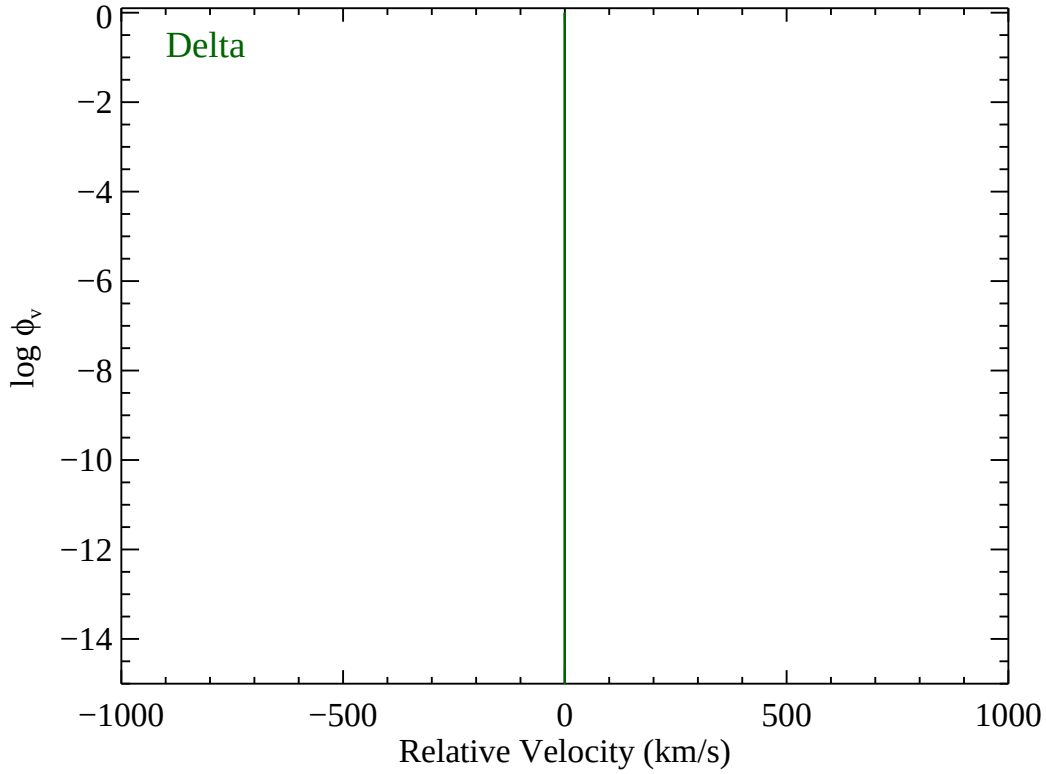

- Natural Broadening (Quantum Mechanics)
  - ◇ Consider the half-life $\tau_{\frac{1}{2}}$ of an excited state

$$\tau_{\frac{1}{2}} = \frac{1}{A_{jk}} \tag{14}$$

    - ▲ Uncertainty principle: $\Delta E \Delta t \sim \hbar$
    - ▲ This implies that the energy of our transition has a finite width
  - ◇ Introduce $W_{jk}(E)$: Characterizes the quantum mechanical probability of a transition occuring between states j and k with energy E
    - ▲ $W(E_j)dE =$ Probability of the lower state being characterized by the energy interval $(E_j, E_j + dE_j)$
    - ▲ $W(E_k)dE =$ Probability of the upper state being characterized by the energy interval $(E_k, E_k + dE_k)$
    - ▲ We are interested in the probability that

$$E \leq E_k - E_j \leq E + dE \tag{15}$$

    - ▲ Convolve

$$W_{jk}(E)dE = \int \int W_j(E_j) W_k(E_k) dE_j dE_k \tag{16}$$

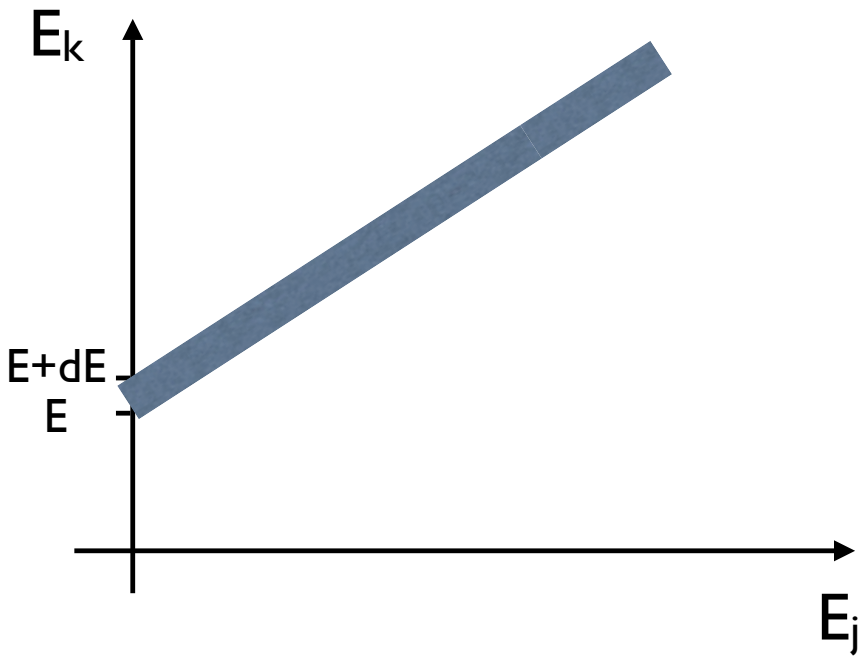

▲ Breit-Wigner profile (Quantum Mechanics)

$$W(E_j)dE_j = \frac{\gamma_j dE_j/h}{(2\pi/h)^2\,[\,E_j - < E_j >\,]^2 + (\gamma_j/2)^2} \tag{17}$$

▲ Gamma value

$$\gamma_j \equiv \sum_{i<j} A_{ij} \tag{18}$$

- For the ground state, there are no levels below
- Therefore, $\gamma_j = 0$

▲ Evaluating $W_{jk}(E)$

$$W_{jk}(E)dE = \frac{[\,\gamma_j + \gamma_k\,]\,dE/h}{(2\pi/h)^2\,[\,E_j - E_{jk}\,]^2 + ([\gamma_j + \gamma_k]/2)^2} \tag{19}$$

▲ Fig

▲ Relating W_{jk} with our cross-section

$$s_\nu = (\text{const})W_{jk}(E)dE \tag{20}$$

- Define: Oscillator strength f_{jk}
  - Value which contains the quantum mechanics
  - Experimentally or theoretically determined
- Finally

$$s_\nu = \frac{\pi e^2}{m_e c} f_{jk} \left[\frac{(\gamma_j + \gamma_k)/4\pi^2}{(\nu - \nu_{jk})^2 + (\gamma_j + \gamma_k)^2/(4\pi)^2} \right] \tag{21}$$

- We can identify the Natural line-profile (normlized to have unit integral value)

$$\phi_N(\nu) = \frac{2}{\pi} \left[\frac{(\gamma_j + \gamma_k)/4\pi^2}{(\nu - \nu_{jk})^2 + (\gamma_j + \gamma_k)^2/(4\pi)^2} \right] \tag{22}$$

- What is the maximum of s_ν?

$$(s_\nu)_{max} = \frac{\pi e^2}{m_e c} f_{jk} \frac{4}{\gamma_j + \gamma_k} \tag{23}$$

  - Compare

$$\frac{s_\nu}{(s_\nu)_{max}} = \frac{\left(\frac{\gamma_j + \gamma_k}{4\pi}\right)^2}{(\nu - \nu_{jk})^2 + \left(\frac{\gamma_j + \gamma_k}{4\pi}\right)^2} \tag{24}$$

  - Define: FWHM = Width where $s_\nu/(s_\nu)_{max} = 1/2$

$$\Delta\nu_{FWHM} = \pm \frac{\gamma_j + \gamma_k}{4\pi} \tag{25}$$

- Finally, return to Lyα
  - $\gamma_1 = 0; \gamma_2 = A_{21} = 6.2 \times 10^8\,\mathrm{s}^{-1}$
  - $\lambda_{21} = 1215.67$Å
  - FWHM

$$\frac{\Delta\lambda_{FWHM}}{\lambda} = \frac{A_{21}}{2\pi\nu_{\mathrm{Ly}\alpha}} = 0.5 \times 10^{-7} \tag{26}$$

$$\Delta\lambda_{FWHM} \approx 6 \times 10^{-5}\,\text{Å} \tag{27}$$

  - Effective Doppler width (see below)

$$(v_D)_{eff} = c \frac{\Delta\lambda_{FWHM}}{\lambda} = 1.5 \times 10^{-2}\,\mathrm{km/s} \tag{28}$$

  - Clearly, true Doppler motions dominate the center of the line profile in the ISM

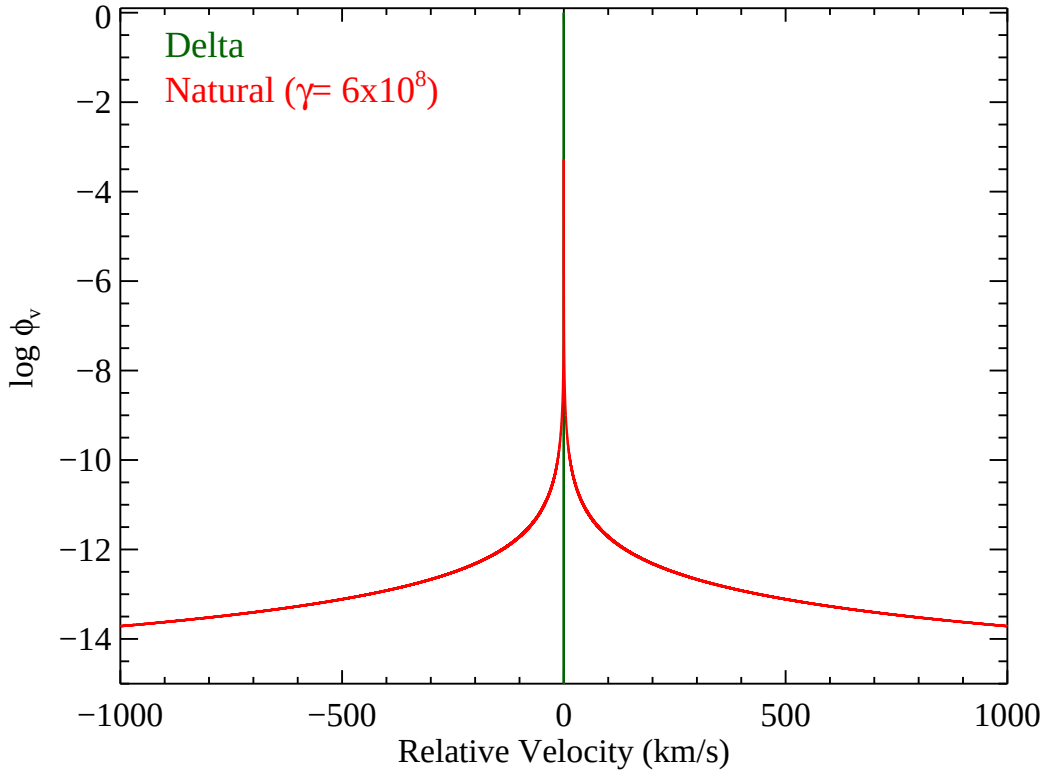

- Doppler Broadening
  - ◇ Each atom in a gas has its own motion ⇒ Doppler
  - ◇ Unique frequency of emission and absorption
  - ◇ This spreads the line out without changing the total amount of absorption
  - ◇ To lowest order in v/c:

$$\nu - \nu_{jk} = \nu_{jk}\frac{v}{c} \tag{29}$$

  - ◇ Adopting a Maxwellian distribution for particles of mass m_A

$$f(v)dv \propto \exp\left(\frac{-m_A v^2}{2kT}\right)dv \tag{30}$$

  - ◇ Profile function

$$\phi_D(\nu) = \frac{1}{\Delta\nu_D\sqrt{\pi}}\exp\left[-\frac{(\nu-\nu_{jk})^2}{\Delta\nu_D^2}\right] \tag{31}$$

$$\Delta\nu_D \equiv \frac{\nu_{jk}}{c}\sqrt{\frac{2kT}{mA}} \tag{32}$$

  - ◇ Line-center ($\nu = \nu_{jk}$) cross-section for each atom (neglecting stimulated

emission)

$$s_0 = B_{jk}\frac{h\nu_{jk}}{4\pi}\phi(\nu_{jk}) \tag{33}$$

$$= \frac{\pi e^2}{mc} f_{jk}\frac{1}{\Delta\nu_D\sqrt{\pi}} \tag{34}$$

- ▲ f_{jk} is the oscillator strength (see above)
- ▲ This describes the quantum mechanical probability of the transition at line-center

◇ Turbulent velocities (macroscopic velocity fields, ξ)

$$\Delta\nu_D = \frac{\nu_{jk}}{c}\left(\frac{2kT}{m_A} + \xi^2\right)^{\frac{1}{2}} \tag{35}$$

◇ Velocity expression for the line-profile

$$\Delta\nu_D \rightarrow b \equiv \sqrt{\frac{2kT}{m_A}} \tag{36}$$

- ▲ Velocity dispersion: σ
- ▲ Doppler parameter: $b = \sigma\sqrt{2}$

$$\phi_D(v) = \frac{1}{b\sqrt{\pi}}\exp\left[-\frac{v^2}{b^2}\right] \tag{37}$$

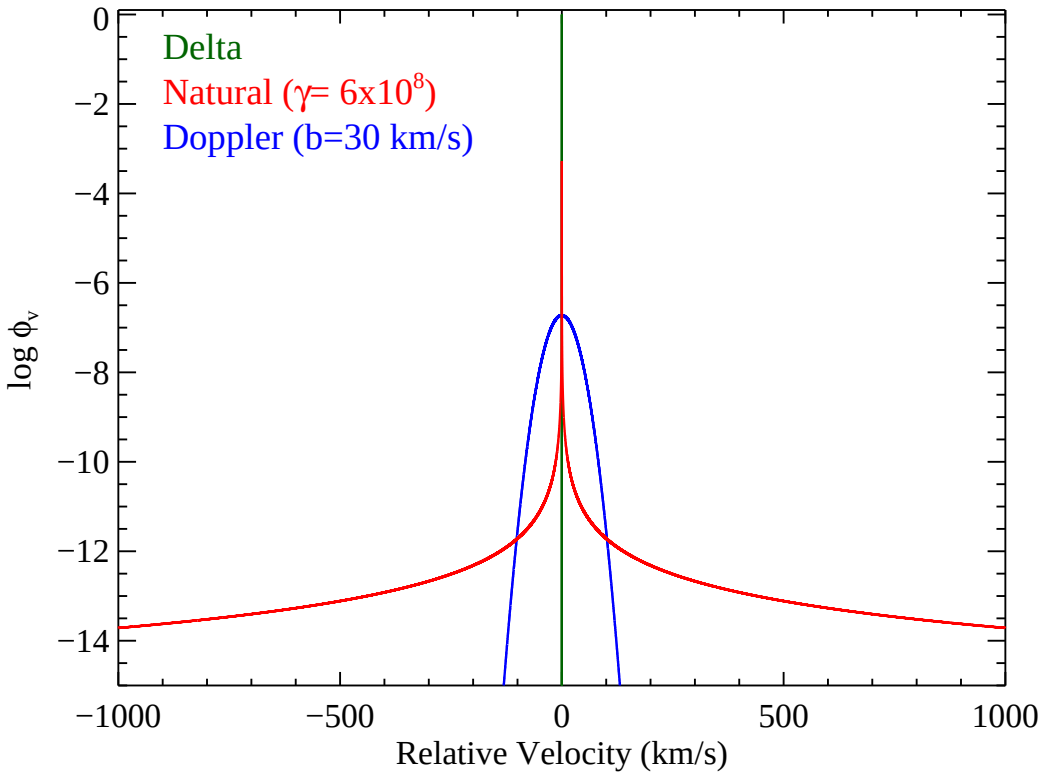

- Voigt profile
  - ◇ Generally, a gas has contributions from Natural and Doppler broadening
    - ▲ Doppler broadening dominates the center profile of the line
    - ▲ The Lorentzian (Natural broadening) dominates the wings

$$\phi(\nu) \propto \frac{1}{(\nu-\nu_0)^2+\gamma^2} \text{ vs. } \exp\left(-\nu^2/\nu_D^2\right) \tag{38}$$

  - ◇ The true profile is a convolution of the two profiles

$$\phi_V(\nu) = \frac{\gamma}{4\pi}\int_{-\infty}^{\infty} \frac{\left(\frac{m}{2\pi kT}\right)^{\frac{1}{2}} \exp\left(-\frac{mv^2}{2kT}\right)}{\left(\nu-\nu_{jk}-\nu_{jk}v/c\right)^2+\left(\gamma/4\pi\right)^2}\,dv \tag{39}$$

  - ◇ Introduce the Voigt function

$$H(a,u) = \frac{a}{\pi}\int_{-\infty}^{\infty} \frac{\mathrm{e}^{-y^2}\,dy}{a^2+(u-y)^2} \tag{40}$$

  - ◇ Identify

$$a \equiv \frac{\gamma}{4\pi\Delta\nu_D} \tag{41}$$

$$u \equiv \frac{\nu-\nu_{jk}}{\Delta\nu_D} \tag{42}$$

  - ◇ Voigt profile

$$\phi_V(\nu) = \frac{H(a,u)}{\nu_D\sqrt{\pi}} \tag{43}$$

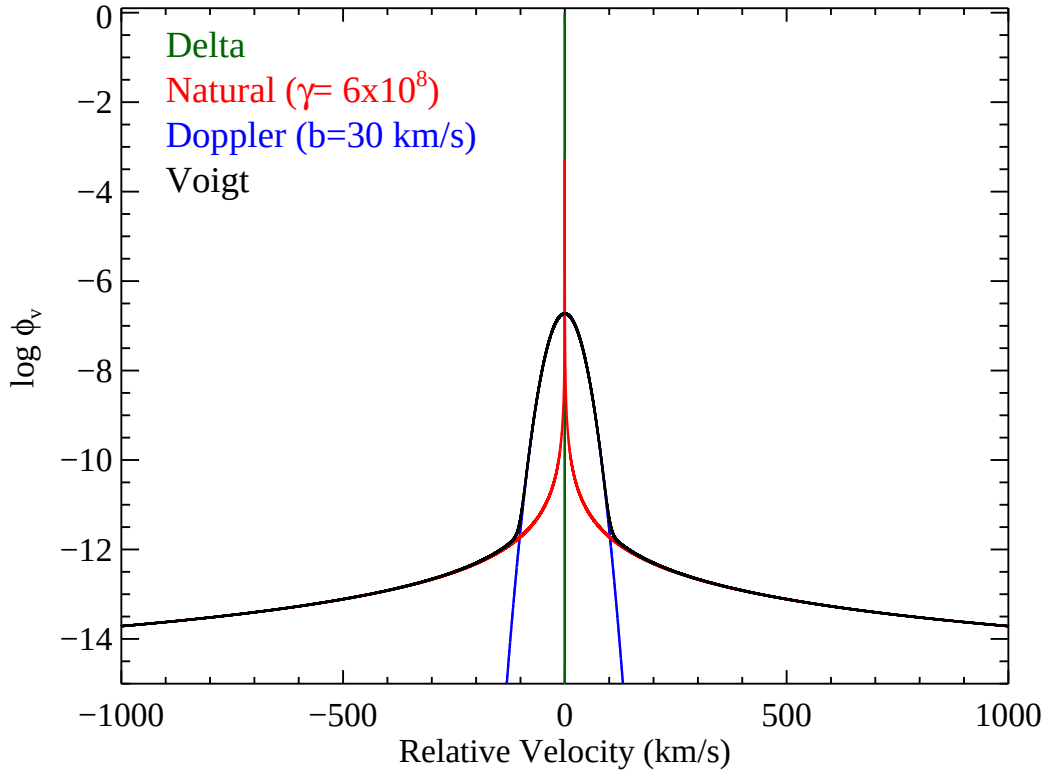

D. Lyα Scattering (A few random points)

- What is the optical depth of Lyα in a typical HII region?
  - ◇ Parameterize in terms of a continuum optical depth

$$\tau_C \equiv \int_0^r n_{\rm HI} \bar{\sigma}\, dr \tag{44}$$

$$\approx n_1 \bar{\sigma}\, r \tag{45}$$

    - ▲ n_1 is the density of atoms in the ground-state
    - ▲ For an HII region, assume $r \approx R_S$ and $\tau_C \approx 1$
    - ▲ Therefore,

$$n_1 \approx \frac{1}{\bar{\sigma} R_S} \tag{46}$$

  - ◇ Consider the optical depth of Lyα at line center τ_0
    - ▲ For a Doppler broadened line, the cross-section at line-center s_0 is given by Eqn 34

▲ This implies an optical depth

$$\tau_0 = \int_0^{R_S} n_1 s_0 \, dr \tag{47}$$

$$\approx \frac{s_0}{\bar{\sigma}} \tau_C \tag{48}$$

$$\approx 0.93 \times 10^4 \left(\frac{T}{10^4 \mathrm{K}} \right)^{-1/2} \tau_C \tag{49}$$

▲ where we took $\bar{\sigma} \approx \sigma_0$

▲ We find $\tau_0 \approx 10^4$ and higher value are possible if the HII region is surrounded by a 'reflecting' HI shell

- What is the escape probability of Lyα from a uniform, spherical HII region?
  - ◇ For any radiation escaping from a uniform cloud of radial depth τ, the escape probability is (without derivation):

$$\epsilon_S(\tau) = \frac{3}{4\tau} \left[1 - \frac{1}{2\tau^2} + \left(\frac{1}{\tau} + \frac{1}{2\tau^2} \right) \mathrm{e}^{-2\tau} \right] \tag{50}$$

  - ◇ For pure Doppler scattering, the probability of emitting a photon at frequency $x = (\nu - \nu_0)/\Delta\nu_D$ is

$$p(x) = \frac{1}{\sqrt{\pi}} \mathrm{e}^{-x^2} \tag{51}$$

  - ◇ If the emission probability and escape probability are uncorrelated, the mean escape probability in the entire line for the whole sphere is:

$$\epsilon(\tau_0) = \int_{-\infty}^{\infty} dx \, p(x) \epsilon_S(\tau_x) \tag{52}$$

$$\tau_x = \tau_0 \mathrm{e}^{-x^2} \tag{53}$$

  - ◇ Remarkably, this integral can be expressed as

$$\epsilon(\tau_0) \approx \frac{1.72}{1.72 + \tau_0} \tag{54}$$

    ▲ The expression is quite accurate for $\tau_0 < 500$

    ▲ And it is ok (to within a factor of 2) for larger τ_0

  - ◇ If Q is the number of scatterings for escape, we have

$$\epsilon(\tau_0) = \frac{1}{1+Q} \tag{55}$$

$$Q = \frac{1}{\epsilon(\tau_0)} - 1 = 5.8 \times 10^3 \ \ (\text{for } \tau_0 = 10^4) \tag{56}$$

- Emission profile
  - ◇ The photons escape in the wings of the line in frequency space, not from the edge of the sphere spatially
    - ▲ That is, they scatter far off line-center ν_0 such that they then 'see' a much smaller cross-section

$$s_x = s_{jk} \mathrm{e}^{-x^2} \tag{57}$$

  - ◇ Photons escape when x is sufficiently large
    - ▲ How large? At $x \approx x_1$ where

$$\tau(x_1) \approx 1 \tag{58}$$

$$\tau(x_1) = \tau_0 \mathrm{e}^{-x^2} = 1 \tag{59}$$

    - ▲ Solving for x_1,

$$\mathrm{e}^{x_1^2} = \tau_0 \tag{60}$$

$$x_1 = \sqrt{\ln \tau_0} \tag{61}$$

  - ◇ For $\tau_0 \approx 10^4$, $x_1 \approx 3$
    - ▲ The majority of photons escape at several times the Doppler width
    - ▲ That is, symmetrically about ν_0 at

$$|\nu - \nu_0| \approx 3 \Delta\nu_D \tag{62}$$

    - ▲ In velocity space, the photons escape at

$$v \approx \pm 3\, b \approx \pm 4\, \sigma_D \tag{63}$$

E. Radiative Transfer in a Diffuse Neutral Medium

- Electric dipole transitions
  - ◇ UV and optical lines
  - ◇ Generally, $h\nu \gg kT$
- Consider a source at distance d with intensity I_ν^* that intersects a cloud with optical depth $\tau_{\nu c}$
  - ◇ Radiative transfer

$$I_\nu = I_\nu^* \mathrm{e}^{-\tau_{\nu c}} + \int_0^{\tau_{\nu c}} \frac{j_\nu}{\kappa_\nu} \mathrm{e}^{-\tau_\nu}\, d\tau_\nu \tag{64}$$

  - ◇ The exponential term in the integral is unimportant (ignore it)
  - ◇ Without derivation, I note that $S_\nu = j_\nu / \kappa_\nu$ is:

$$S_\nu \approx \epsilon B_\nu(T) + (1 - \epsilon) \int d\nu\, \phi_\nu J_\nu \tag{65}$$

- ▲ The first term is due to thermal emission. It is insignificant when $kT \ll h\nu$
- ▲ The second term is due to scattering

- Consider scattering further
  (a) Scattering of the source

$$J_\nu^* = \frac{1}{4\pi}\int I_\nu^*\, d\Omega \tag{66}$$
$$= \frac{\Omega^*}{4\pi} I_\nu^* \tag{67}$$
$$\approx \left(\frac{R_s}{d}\right)^2 I_\nu^* \tag{68}$$
$$\approx 10^{-20} I_\nu^* \tag{69}$$

  (b) Scattering of ambient radiation (photons from all sources)
  - ◇ Energy density of the ISM ($T_{eq} \approx 3$K)

$$u = aT_{eq}^4 \tag{70}$$

  - ◇ Ambient intensity

$$J_\nu \sim \frac{uc}{4\pi\nu} \tag{71}$$

  - ◇ Source intensity (stellar)

$$I_\nu^* = \frac{aT_*^4 c}{4\pi\nu} \tag{72}$$

  - ◇ Combining

$$J_\nu = \left(\frac{T_{eq}}{T}\right)^4 I_\nu^* \tag{73}$$
$$\sim 10^{-13} I_\nu^* \tag{74}$$

- We conclude that scattering is irrelevant too
- Therefore, our radiative transfer simplifies to

$$I_\nu = I_\nu^* \mathrm{e}^{-\tau_\nu} \tag{75}$$

- We can now consider the formation of absorption lines as a simple integration of the optical depth

F. Equivalent Width

- Definition: W_λ is the gross measure of the flux absorbed (scattered) by the gas cloud
  - ◇ It is the convolution of the optical depth with the line profile
  - ◇ This is primarily an observational quantity
  - ◇ Conveniently, it is *independent* of the instrument profile

◇ For a normalized-flux absorption line, it is simply the area above the curve

- Example

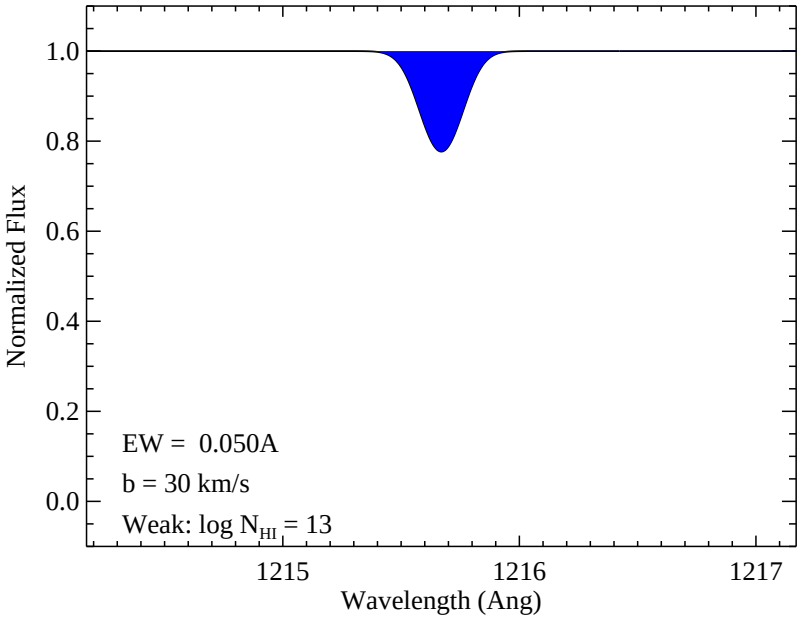

- Numerically

$$W_\lambda = \int_0^\infty \left[1 - \frac{I_\nu}{I_\nu^*} \right] d\lambda \tag{76}$$

◇ I_ν is the observed intensity and I_ν^* is the intensity of the source

◇ Substituting the transfer equation for the ISM

$$W_\lambda = \int_0^\infty [\, 1 - \exp(-\tau_\lambda) \,] \, d\lambda \tag{77}$$

◇ Constrast this equation with analysis of stellar atmospheres (they have a very different radiative transfer equation)

- Inserting our optical depth equation

◇ Assume a constant (or average) opacity for the cloud

$$\tau_\lambda = \int \kappa_\lambda \, ds \tag{78}$$

$$= \int \sigma_\lambda n_j ds \tag{79}$$

$$= \frac{\pi e^2}{m_e c^2} \lambda_{jk}^2 f_{jk} \phi_\lambda N_j \tag{80}$$

◇ where we have introduced the column density

$$N_j \equiv \int n_j \, ds \tag{81}$$

G. Curve of Growth (Theory)

- Definition
  - ◇ The curve-of-growth (COG) relates the optical depth of a line with the equivalent width of that absorption feature
  - ◇ In brief, it describes the transition from a Doppler dominated line to a naturally broadened line
- Consider three 'limits'

(a) Weak line limit ($\tau_0 \ll 1$)

- ◇ Natural broadening is negligible
- ◇ Doppler broadening dominates

$$\tau_0 = \frac{\pi e^2}{m_e c} f_{jk} N_j \left(\frac{1}{\sqrt{\pi}\Delta\nu_D} \right) \tag{82}$$

- ◇ With τ_0 small, our equation for the equivalent width becomes

$$W_\lambda = \frac{\lambda^2}{c} \int [\, 1 - \exp(-\tau_\nu) \,]\, d\nu \tag{83}$$

$$\approx \frac{\lambda^2}{c} \int_0^\infty \tau_\nu \, d\nu \tag{84}$$

$$= \frac{\lambda^2}{c} \frac{\pi e^2}{m_e c} f_{jk} N_j \tag{85}$$

$$= \lambda^2 f_{jk} N_j \, (8.85 \times 10^{-13}) \tag{86}$$

- ◇ This is the 'linear' portion of the curve-of-growth

$$W_\lambda \propto N_j \tag{87}$$

- ◇ See the previous figure for an example
- ◇ In this limit, $W_\lambda \ll 1$Å

(b) Strong line limit ($\tau_0 > 1$)

- ◇ Again, ignoring natural broadening

$$\tau_x = \tau_0 \mathrm{e}^{-x^2} \tag{88}$$

- ▲ $x \equiv \Delta\nu / \Delta\nu_D$
- ▲ Consider $x_1 \equiv \sqrt{\ln \tau_0}$
- ▲ For $|x| < x_1$, $I_\nu \ll I_\nu^*$
- ▲ Therefore,

$$W \propto 2x_1 \approx 2\sqrt{\ln \tau_0} \tag{89}$$

- ◇ To change W_λ in this limit, we need to increase τ_0 immensely

◇ Example

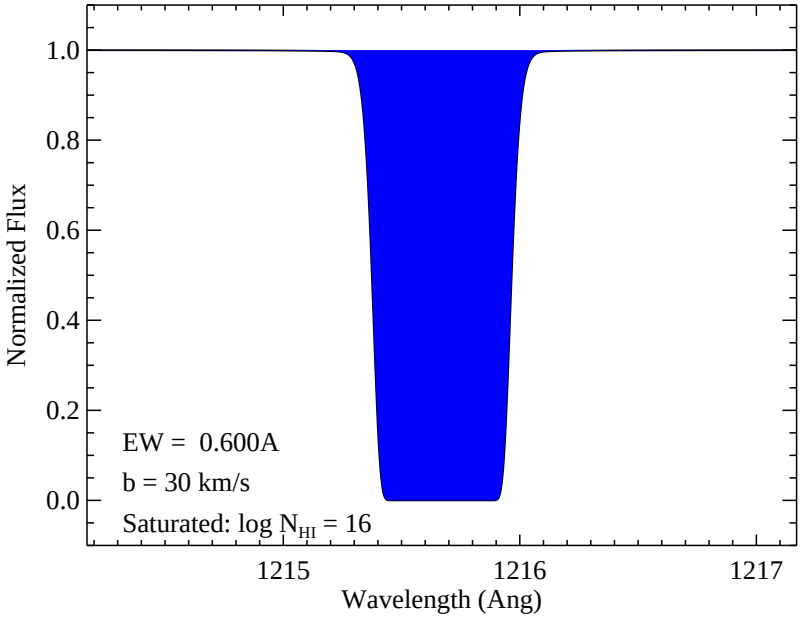

◇ Analytically

$$W_\lambda = \frac{\lambda^2}{c}\Delta\nu_D \int_{-\infty}^{\infty} dx \left[1 - \mathrm{e}^{-\tau_0 \mathrm{e}^{-x^2}}\right] \tag{90}$$

▲ Evaluate numerically

▲ Express as

$$\frac{W_\lambda}{\lambda} = \frac{2v_D}{c} F(\tau_0) \tag{91}$$

▲ Table

Table 1: SOME $F(\tau_0)$ VALUES

τ_0	0.000	0.100	0.300	0.500	0.800
$F(\tau_0)$	0.000	0.086	0.240	0.374	0.545
τ_0	1.000	1.400	2.000	3.000	6.000
$F(\tau_0)$	0.643	0.804	0.986	1.188	1.483
τ_0	10.00	20.00	30.00	60.00	100
$F(\tau_0)$	1.66	1.86	1.97	2.14	2.26
τ_0	1000	10000			
$F(\tau_0)$	2.73	3.12			

▲ In the limit that $\tau_0 \gg 1$,

$$F(\tau_0) = [\ln \tau_0]^{\frac{1}{2}} \tag{92}$$

▲ In this Strong line limit, W_λ is insensitive to τ_0 and most sensitive to the internal structure of the cloud

$$W_\lambda \propto v_D \tag{93}$$

▲ Figure (red = 10km/s, green=20km/s)

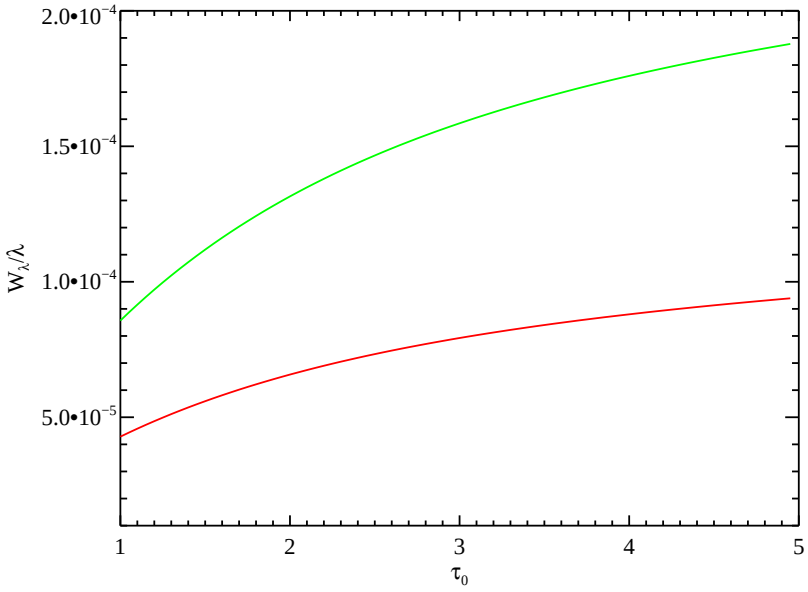

- ○ Note the small change in W_λ with increasing τ_0
- ○ And the linear sensitivity to ν_D

(c) Damping limit ($\tau_0 \gg 1$)

- ◇ Natural broadening is now important

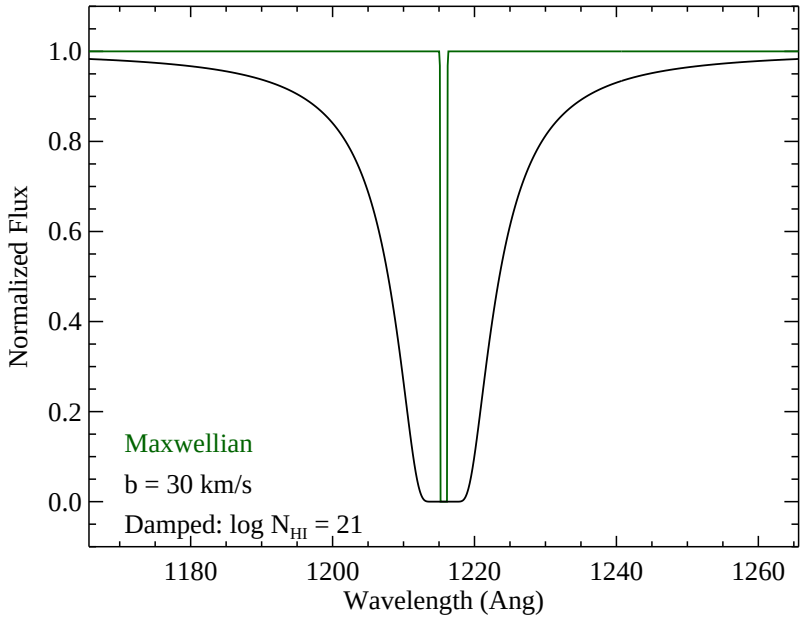

◇ Optical depth (Lorentzian profile)

$$\tau_x \approx \frac{\tau_0 A}{\sqrt{\pi}} \frac{1}{x^2} \tag{94}$$

$$A = \frac{\gamma_j + \gamma_k}{4\pi} \tag{95}$$

◇ Setting $\tau_x = 1$,

$$x_1 = [\,\tau_0 A\,]^{\frac{1}{2}} \tag{96}$$

◇ Therefore,

$$W_\lambda \propto 2x_1 \propto N^{\frac{1}{2}} \tag{97}$$

◇ Formally

$$\frac{W_\lambda}{\lambda} = \frac{2}{c}\left[\lambda^2 N_j \frac{\pi e^2}{m_e c} f_{jk} A\right]^{\frac{1}{2}} \tag{98}$$

- Example COG: Lyα lines with a wide range of column density (τ_0)

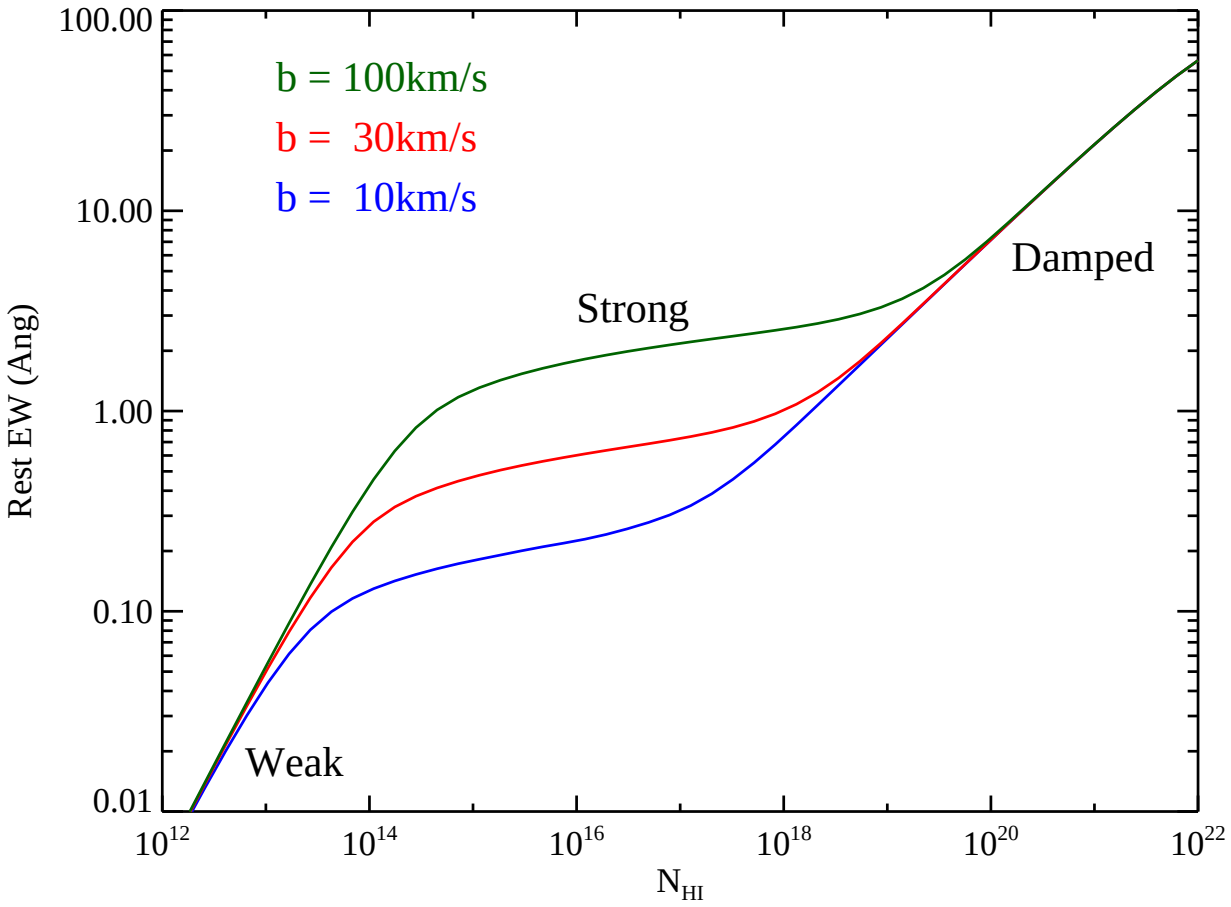

H. Notation

- Ions and Atoms
  - ◇ Express as the element with the ionization state super-scripted
  - ◇ Examples
    - ▲ C^0 is atomic carbon
    - ▲ C^+ is singly ionized carbon
  - ◇ Column density: $N(C^+)$
- Resonance transitions
  - ◇ Definition: Electric dipole transitions from the ground-state
  - ◇ Label the ionization state with Roman numerals
  - ◇ Label the vacuum wavelength as a whole number (rounding optional)
  - ◇ Examples
    - ▲ CI 1560
    - ▲ CII 1334
  - ◇ Warning: Often people write column densities as $N(\mathrm{CII})$
- Fine-structure transitions
  - ◇ Electric dipole transitions from an excited state
  - ◇ There is no agreed upon notation
  - ◇ Generally, these are labelled with a * (or two)
    - ▲ CI** 1561
    - ▲ CII* 1335

I. Column Densities

- Definition

$$N_j = \int n_j \, ds \tag{99}$$

  - ◇ Simple counting of atoms per cm^{-2}
  - ◇ Analagous to analyzing a core sample from the Earth
    - ▲ But without explicit distance information
    - ▲ Only velocity resolution, $\delta v = c\,\delta\lambda/\lambda$
- Physical importance
  - ◇ Endless...
  - ◇ Metallicity, e.g. O/H
  - ◇ Chemical abundances, e.g. O/Fe
  - ◇ Dust depletion (see next lecture)
  - ◇ Ionization conditions, e.g. C^0/C^+
  - ◇ Studies of the ISM, IGM, etc.

- Measuring column densities
  - ◇ Curve of Growth
    - ▲ Previously, we described the COG as a theoretical relationship between W_λ and τ_0
    - ▲ But, recall

$$\tau_0 = \frac{\pi e^2}{m_e c} f_{jk} N_j \left(\frac{1}{\sqrt{\pi}\Delta\nu_D} \right) \tag{100}$$

$$= \frac{\sqrt{\pi} e^2}{m_e c} \frac{\lambda_{jk} f_{jk} N_j}{b} \tag{101}$$

$$= 1.497 \times 10^{-2} \frac{\lambda_{jk} f_{jk} N_j}{b} \tag{102}$$

$$\tag{103}$$

    - ▲ Basic idea
      - ○ For a series of transitions from the same ion, t he column density N_j and Doppler parameter b are constant but $f_{jk}\lambda_{jk}$ varies, i.e.

$$\tau_0 \propto f_{jk}\lambda_{jk} \tag{104}$$

      - ○ One measures W_λ as a function of $f\lambda$ to fit for N, b
    - ▲ Key assumption
      - ○ Generally assume a single cloud (i.e. one b value)
      - ○ But, see Jenkins 1986
    - ▲ Advantages of COG technique
      - ○ One uses only W_λ measurements, i.e. low-resolution data is fine
      - ○ Results are independent of the instrumental line-spread function
      - ○ Can include multiple ions (assuming they have the same intrinsic line-profiles)
    - ▲ Disadvantages of COG technique
      - ○ The universe is rarely as simple as a single cloud
      - ○ Can easily underestimate N significantly (e.g. Prochaska 2006)
      - ○ Requires a large dynamics range in $f\lambda$ values
      - ○ W_λ estimates can be model dependent
    - ▲ Example: HI Lyman series
      - ○ Lyα ($n = 1$ to 2): $f\lambda = 506.2$Å
      - ○ Ly-15 ($n = 1$ to 16): $f\lambda = 0.353$Å
      - ○ Observe W_λ and analyze against $f\lambda$
      - ○ Fit for N and b

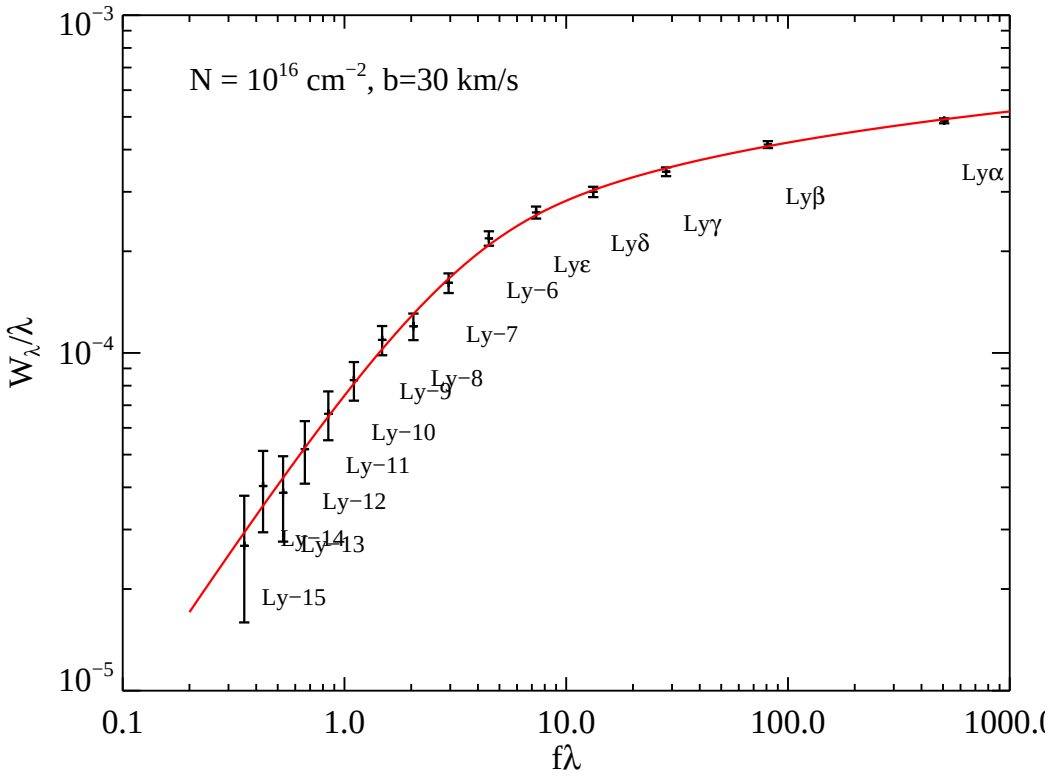

◇ Line-profile fitting

▲ Concept

- Model the data as 'clouds' with unique velocity, column density and Doppler parameters
- Add up the optical depths as a function of frequency and convolve with the instrument line-spread function
- Perform least-squares analysis on the parameters

▲ Advantages

- Makes use of all the pixels in the data
- Allows for complicated (i.e. multiple cloud) models

▲ Disadvantages

- Requires good knowledge of the line-spread function
- Results may depend on initial guess at the model (e.g. the number of 'clouds')
- Labor/computationally intensive

▲ Software packages

- VPFIT (http://www.ast.cam.ac.uk/∼rfc/vpfit.html)
- MIDAS

▲ Examples

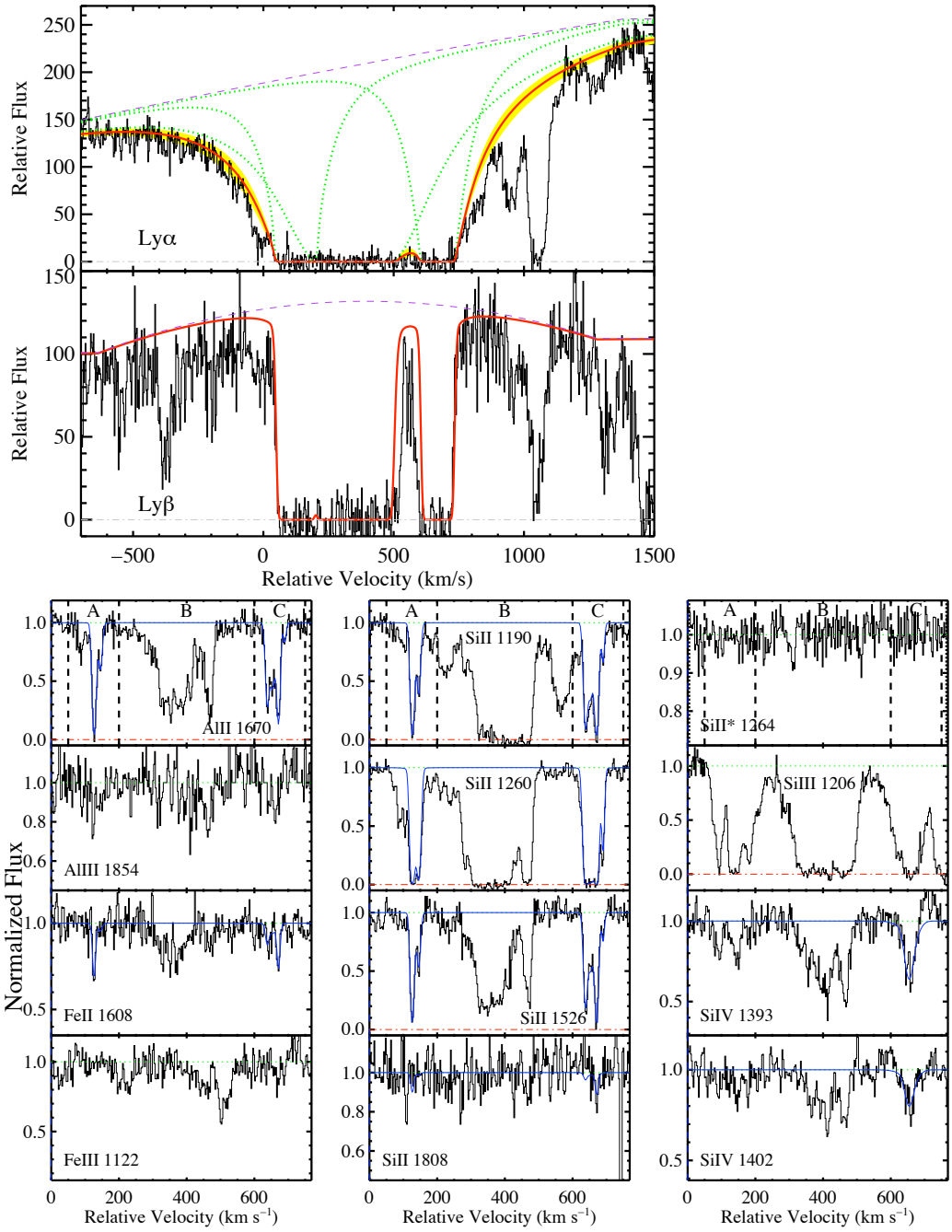

◇ Other techniques

▲ Apparent Optical Depth Method

○ Useful for resolved data (high-resolution)

○ Savage & Sembach (1991)

○ Jenkins (1996)

▲ ??

J. Applications: D/H

- Motivations
  - ◇ At $t \sim 1$min in the early universe, the free protons and neutrons fuse to form ^{4}He and trace amounts of D, B, Be, Li
  - ◇ This process of Big Bang Nucleosynthesis (BBN) is the only channel for producing D
    - ▲ All astrophysical processes destroy D
    - ▲ e.g. stellar nucleosynthesis
  - ◇ Therefore, a measurement of D/H in a primordial gas (i.e. one free of astrophysical processes) probes the physics of the early universe
  - ◇ In particular, one can constrain the baryonic mass density Ω_b
- A brief summary of BBN
  - ◇ Definition: Epoch in the universe when the temperature drops below $T \approx 10^{10}$K so that free p,n fuse to form He and other light nuclei
  - ◇ Given $T = 3$K and $H_0 \approx 70\,\mathrm{km/s/Mpc}$, we estimate $t_{BBN} \approx 5$min after the Big Bang
  - ◇ Formation of ^{4}He

$$\mathrm{p} + \mathrm{n} \rightarrow \mathrm{D} \tag{105}$$

$$\mathrm{D} + \mathrm{D} \rightarrow {}^3\mathrm{He} + \mathrm{n} \tag{106}$$

$${}^3\mathrm{He} + \mathrm{D} \rightarrow {}^4\mathrm{He} + \mathrm{p} \tag{107}$$

    - ▲ For the light elements, ^{4}He is by far the most energetically favorable
    - ▲ Nearly all free n are incorporated into ^{4}He
  - ◇ Other light elements and isotopes (D, Li, ^{3}He)
    - ▲ Thermodynamics: Competition between lowest energy state and higher entropy
    - ▲ Higher entropy implies more unique states, i.e. production of elements/isotopes other than ^{4}He
  - ◇ Entropy of the universe can be characterized as the photon to baryon ratio, n_γ/n_b
    - ▲ Introduce the inverse quantity

$$\eta \equiv \frac{n_b}{n_\gamma} \tag{108}$$

    - ▲ Higher η means lower entropy
    - ▲ Higher η implies more D, Li, Be relative to He (or H)
  - ◇ BBN halts before producing Carbon and heavier elements
    - ▲ High entropy limits C formation
    - ▲ Very few 'stepping stones' to produce C (Li, Be are rare)

- ▲ C production generally requires a 3-body interaction (three ^{4}He nuclei)
- ▲ Expansion of the universe drops T before significant C is produced

◇ Figure

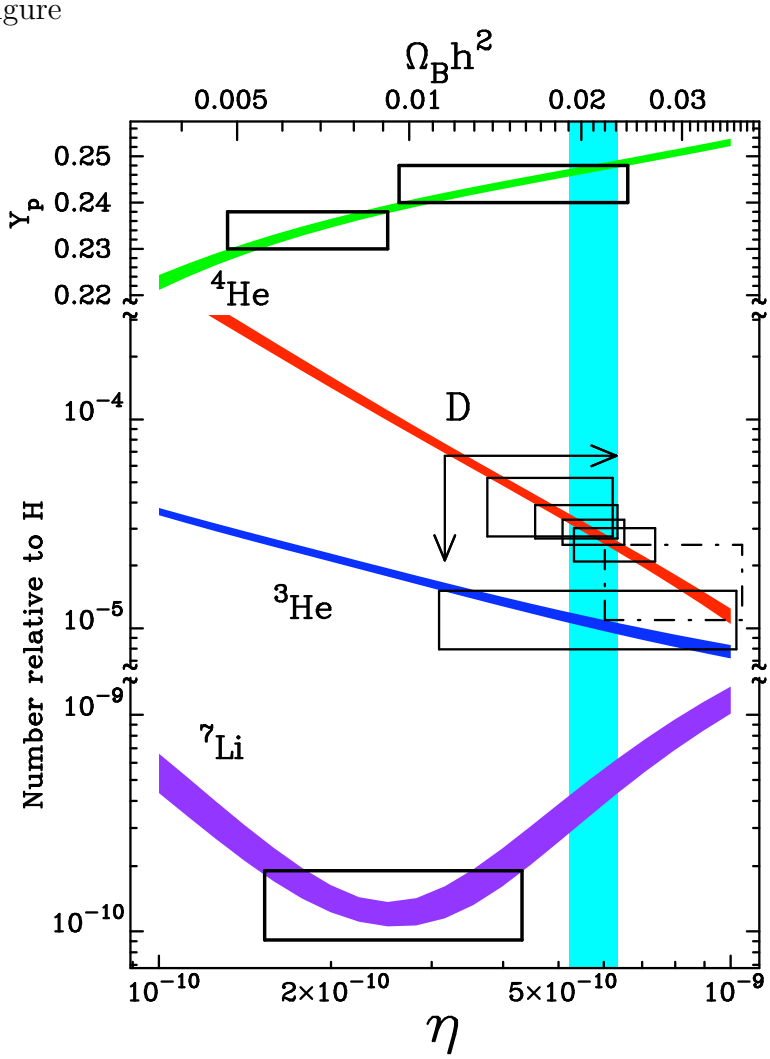

- ▲ The curves are theoretical predictions for each isotope relative to H
- ▲ It is apparent from the figure, that D/H is the most sensitive to η

- Experiment
  - ◇ Measure D/H in a primordial gas
  - ◇ Compare against the theoretical prescription for BBN
  - ◇ Infer η to predict Ω_b (we know n_γ from the CMB)
- Observations
  - ◇ Count atoms in a 'primordial' cloud
    - ▲ Distant (high z, i.e. far back in time as possible)
    - ▲ Metal-poor (avoid stellar nucleosynthesis)
    - ▲ Preferably outside of a galaxy

- ◇ Analyze the Lyman series in absorption to measure column densities
- ◇ Use quasar absorption line (QAL) spectroscopy
  - ▲ The quasar is not physically associated with the gas
  - ▲ It is a convenient background source for studying the cloud

- Example (O'Meara et al. 2006)

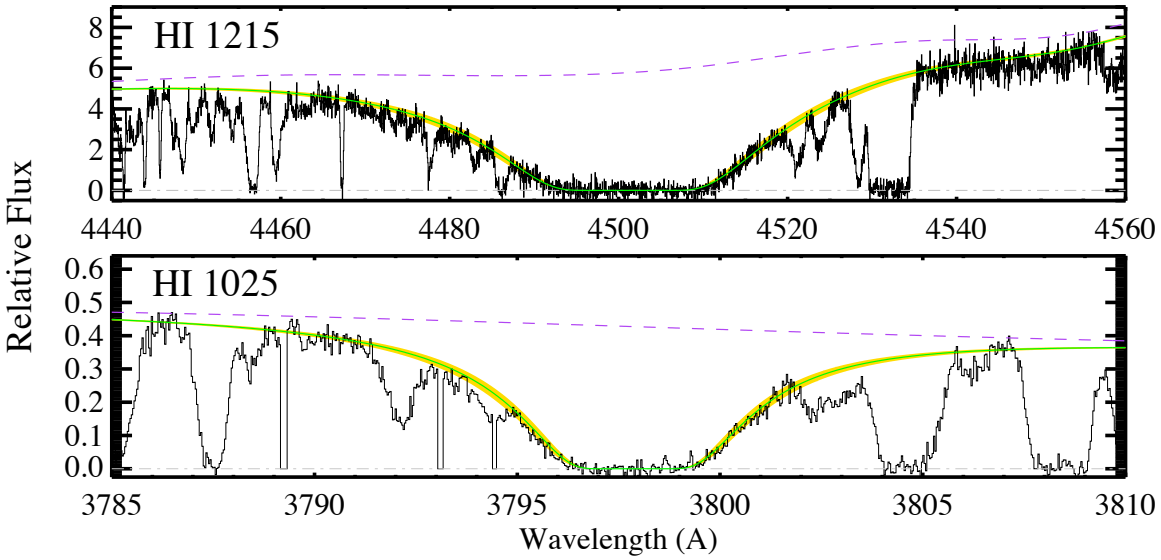

- ◇ Gas cloud at $z = 2.7$ toward J1558–0031
- ◇ Hydrogen
  - ▲ The Lyα and Lyβ lines are damped ($W_\lambda \propto N_{\rm HI}^{\frac{1}{2}}$)
  - ▲ Fitting a Voigt profile to the data yields a precise measure of $N_{\rm HI}$
    - ○ In principle, every pixel constrains $N_{\rm HI}$
    - ○ But, the unknown 'continuum' I_ν^* and Lyα absorption from coincident, unrelated clouds introduce dominant, systematic error
  - ▲ The overplotted curve and shaded region corresponds to

$$\log(N_{\rm HI}/\,{\rm cm}^{-2}) = 20.67 \pm 0.05 \tag{109}$$

- ◇ How do we measure D?
  - ▲ Freshman physics tells us that the energy shift due to the additional neutron (via the reduced mass μ) is:

$$\frac{\Delta E}{E} = \frac{E_D - E_H}{E_H} \tag{110}$$

$$= \frac{\mu_D}{\mu_H} - 1 \tag{111}$$

$$= 2.7 \times 10^{-4} \tag{112}$$

  - ○ In velocity (negative for higher energy)

$$\Delta v \;=\; c\,\frac{\Delta E}{E} \;=\; -82\,{\rm km/s} \tag{113}$$

- But this implies the Lyα line for DI is deep within the core of the Lyα (and Lyβ) lines of HI

▲ Furthermore, if D/H $\approx 10^{-5}$

- This implies absorption on the saturated portion of the COG
- i.e. a line without sensitivity to the $N_{\rm DI}$

▲ Solution: Choose higher order lines in the Lyman series

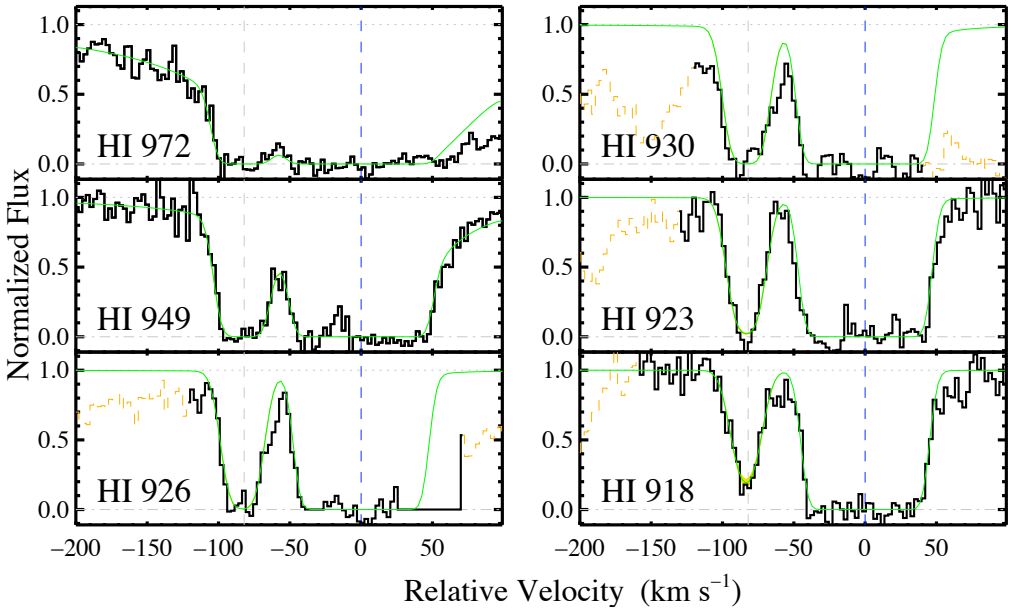

◇ DI

▲ At Ly-11 (HI 918), we have

$$(f\lambda)_{\rm Ly-11} = 0.00167\,(f\lambda)_{\rm Ly\alpha} \tag{114}$$

▲ The HI lines now lie on the saturated portion of the COG (no damping wings)

▲ And for D/H $\approx 10^{-5}$, this implies DI absorption on the weak portion of the COG

$$W_\lambda \propto N_{\rm DI} \tag{115}$$

▲ Measuring D is therefore trivial

$$\log(N_{\rm DI}/\,{\rm cm}^{-2}) = 16.19 \pm 0.04 \tag{116}$$

- D/H

◇ The strength of absorption line analysis is that abundance ratios are determined simply by comparing column densities

$$\frac{\rm D^0}{\rm H^0} = \frac{N_{\rm DI}}{N_{\rm HI}} \tag{117}$$

◇ But, are we finished? We wanted D/H, not $\rm D^0/H^0$!

▲ What if the gas is highly ionized?

- ▲ Or what if the D and H is locked up in dust? (we only measure gas)
- ▲ And is it primordial?

◇ Ionization?

- ▲ Charge exchange reactions keep $D^0/H^0 = D/H$
- ▲ Specifically,

$$D^+ + H^0 \leftrightarrow D^0 + H^+ \tag{118}$$

◇ Depletion?

- ▲ D may deplete more readily into dust than H (see Prochaska et al. 2005, Draine 2006)
- ▲ But the depletion should be small in this gas

◇ Primordial?

- ▲ High redshift ($z = 2.7$)
- ▲ Metal poor
  - ○ Measuring O^0 from OI 1302: $N(O^0) = 10^{15.86}\,cm^{-2}$
  - ○ $O/H = O^0/H^0 = 10^{-4.8} = 0.04\ (O/H)_\odot$
  - ○ Very little D will have been processed by stars

◇ Final answer

$$\frac{D}{H} = 10^{-4.48\pm0.06} \tag{119}$$

- Current measurements

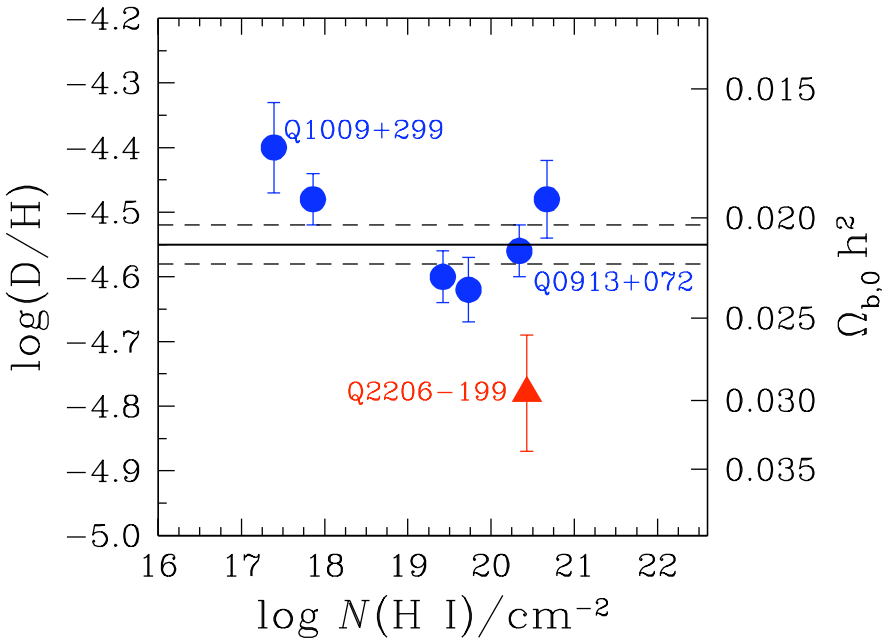

◇ Pettini et al. 2009

◇ Simple statistics

$$< \log D/H >= -4.55 \pm 0.03 \tag{120}$$

- ◇ The scatter appears larger than the estimated variances
  - ▲ Variations in D/H throughout the universe? (unlikely)
  - ▲ Underestimated errors by the observers? (likely)

- Cosmology
  - ◇ Using this <D/H> value and BBN theory

$$\Omega_b^{\rm BBN} h^2 = 0.0213 \pm 0.0010 \tag{121}$$

  - ◇ This agrees extremely well with the baryon density estimate from the CMB (WMAP; Dunkley et al. 2008)

$$\Omega_b^{\rm CMB} h^2 = 0.02273 \pm 0.00062 \tag{122}$$

  - ◇ Triumph of physics + astrophysics

K. Applications: Lyα Forest

- Motivations
  - ◇ Study gas between galaxies in the distant universe
  - ◇ Constrain the dark matter power spectrum
  - ◇ Investigate feedback processes from galaxies (e.g. metal enrichment)
  - ◇ Constrain the ambient UV radiation field
  - ◇ And much much more..
- Definition: Lyα line opacity in the spectrum of a distant source due to HI gas in the foreground (at lower z)
  - ◇ Originally discovered in the spectra of quasars
  - ◇ Now also observed in galaxies and GRB afterglows
  - ◇ Also known as the Intergalactic Medium (IGM)
- Example

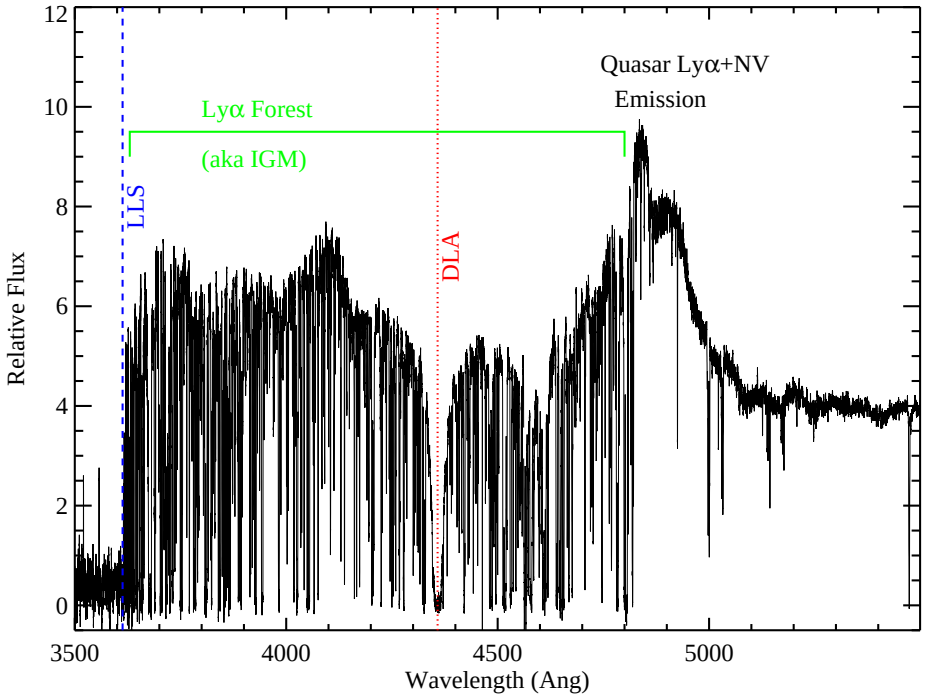

- Quasar continuum (I_ν^*)
  - ◇ Dominant source of uncertainty in many analyses, e.g. $W \propto (1 - I_\nu/I_\nu^*)$
  - ◇ The quasar spectrum is characterized by a power-law

$$f_\nu \propto \nu^{-1.6} \tag{123}$$

  - ◇ And strong emission lines like Lyα, CIV, OVI, [CIII]
    - ▲ The quasar continuum may have contributions from strong/weak emission lines at all wavelengths
    - ▲ Nearly impossible to predict the continuum I_ν^* within the Lyα forest
- Immediate result: Reionization
  - ◇ The fact that we observe a single photon at wavelengths below the rest-frame Lyα of the quasar indicates the universe is highly ionized
  - ◇ Mean Hydrogen number density: $\bar{n}_{\rm H}$

$$\bar{n}_{\rm H}(z) = \Omega_b \rho_c (1+z)^3/(m_p \mu) \tag{124}$$

    - ▲ ρ_c is the critical density:

$$\rho_c \equiv \frac{3H_0^2}{8\pi G} = 1.88 \times 10^{-29} h^2 \ ({\rm g/cm^3}) \tag{125}$$

    - ▲ μ is the reduced mass which mainly accounts for He ($\mu = 1.3$)
    - ▲ $(1+z)^3$ simply accounts for expansion of the universe

▲ Note that the h^2 terms cancel between our measurement of Ω_b and ρ_c

$$n_{\rm H}(z) = 1.84 \times 10^{-7} (1+z)^3 \quad \text{atoms/cm}^3 \tag{126}$$

◇ Consider a small path ℓ through the Universe, such that the velocity width from Hubble expansion is small (< 100km/s)

$$\delta v \approx H\ell \tag{127}$$

▲ At $z = 3$, $H \approx 100$km/s/Mpc

▲ Take $\ell = 0.1$Mpc

◇ The H column density at $z = 3$ for such a patch is:

$$N_{\rm H} = n_{\rm H}\ell \tag{128}$$

$$= 3.6 \times 10^{18}\,\text{cm}^{-2} \tag{129}$$

◇ If this gas is neutral, i.e. $N_{\rm HI}$= $N_{\rm H}$, the line-center opacity from Lyα is:

$$\tau_0 = 1.497 \times 10^{-2} \frac{\lambda_{jk} f_{jk} N_j}{b} \tag{130}$$

$$= 7.6 \times 10^{-13} \frac{N_{\rm H}}{b[\text{km/s}]} \tag{131}$$

$$= 2.7 \times 10^5 \frac{N_{\rm H}}{3.6 \times 10^{18}\,\text{cm}^2} \frac{10\,\text{km/s}}{b} \tag{132}$$

▲ If the universe where even near neutral ($n_{\rm HI}/n_H > 10^{-3}$), not a single Lyα photon would transmit to Earth

▲ The observations of the Lyα forest rules out such a Gunn-Peterson trough at $z = 3$

◇ To wit,

▲ Reionization!

▲ We infer an extragalactic UV background (EUVB) radiation field which ionizes 99% of the universe

- Observational characterization of the Lyα forest (traditional)

◇ Describe the opacity as a set of individual absorption lines

▲ Observationally motivated

▲ But also physical – view the lines as 'clouds' at unique redshifts

◇ Equivalent widths

▲ Standard, observational analysis

▲ Results (Sargent et al. 1981, ApJS, 42, 41)

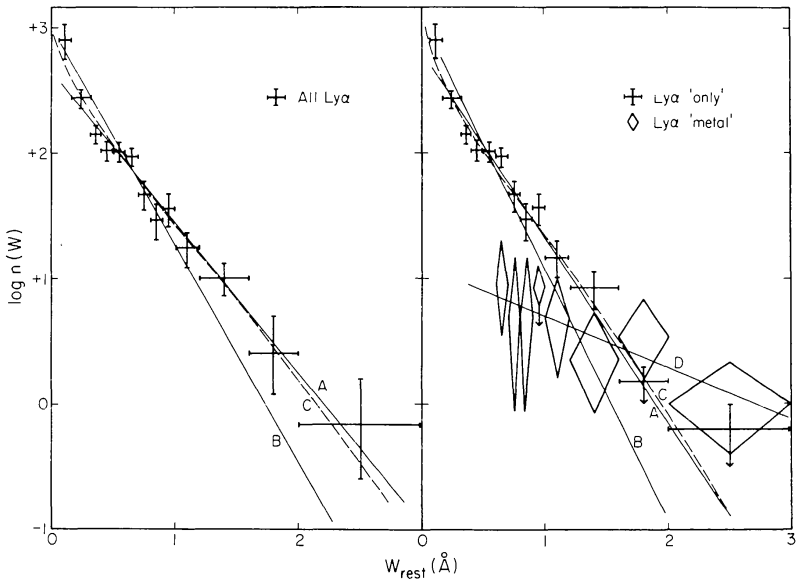

- $n(W)$ is the number of lines with rest equivalent width in the interval $(W, W + dW)$
- Parameterize as

$$n(W) = \frac{N^*}{W^*} \exp(-W/W^*) \tag{133}$$

- Maximum likelihood analysis gives

$$N^* = 154 \pm 11 \tag{134}$$

$$W^* = 0.362 \pm 0.021 \text{ Å} \tag{135}$$

▲ W_λ values are useful for searching for redshift evolution, but have minimal intrinsic physical meaning

◇ Column density and Doppler width distributions

▲ Fit Voigt profiles to high resolution data to determine $z, N_{\rm HI}, b$

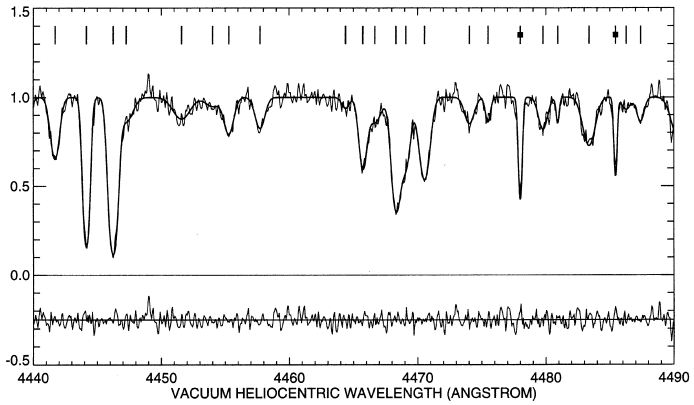

FIG. 1. A sample 50 Å region of the spectrum of Q0302−003 showing fits to identified lines overlaid upon the normalized spectrum. Residuals to the fits are shown below, and it can be seen that there are no systematic residuals associated with the profile fits. The wavelengths of each line are marked by ticks above the spectrum. There are two lines with b<14 km s^{-1} in this region of spectrum where the ticks are overlaid by boxes. These lines correspond to a C IV doublet at z=1.892 (Table 2) and are easily distinguished from the broader forest lines. The number of lines fitted for each quasar is summarized in Table 1.

- Extremely time-consuming
- Subject to analysis bias (e.g. initial guesses)

▲ Doppler parameter distribution ($z \approx 3$; Kirkman & Tytler 1997)

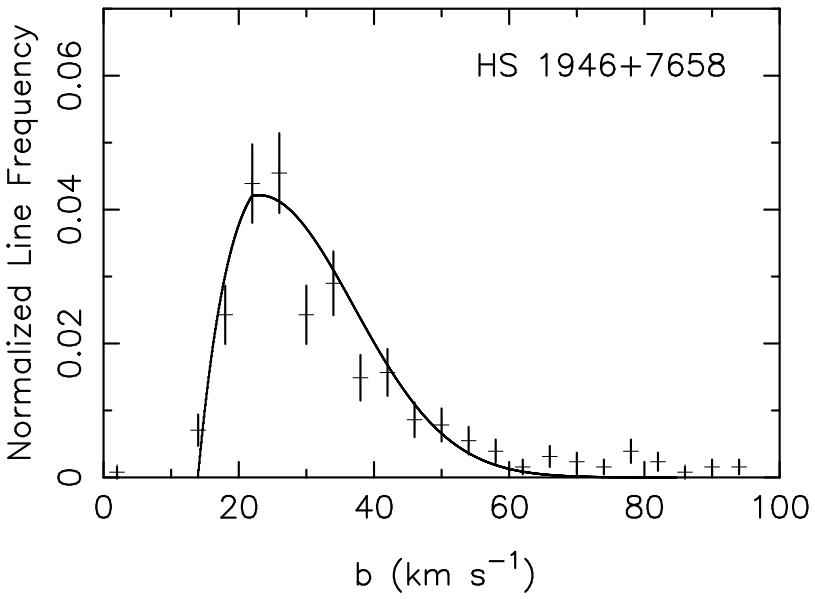

FIG. 4.—Observed b distribution toward HS 1946+7658. The lines have been binned into intervals of 4 km s^{-1} in b. The vertical bars represent 1 σ errors. The curve is our best estimate of the intrinsic b distribution—a Gaussian with mean 23 km s^{-1}, $\sigma_b = 14$ km s^{-1}, and $b_{\rm min}$ given by eq. (4). We believe that most of the lines with $b < 14$ km s^{-1} are not part of the intrinsic b distribution. The lines with $b > 60$ km s^{-1} are probably real, but some must be blends and some may be continuum errors. The sum of all line frequencies is 1.

- Note the cutoff at $b \approx 20\,\mathrm{km/s}$
- One may interpret this as the temperature of the IGM

$$b = \left(\frac{2kT}{m_A} + \xi^2 \right)^{\frac{1}{2}} \tag{136}$$

- Taking $\xi = 0$, $T_{\rm IGM} = 25,000\mathrm{K}$
- This remains one of the 'better' ways to estimate $T_{\rm IGM}$

▲ Column densities (frequency distribution)

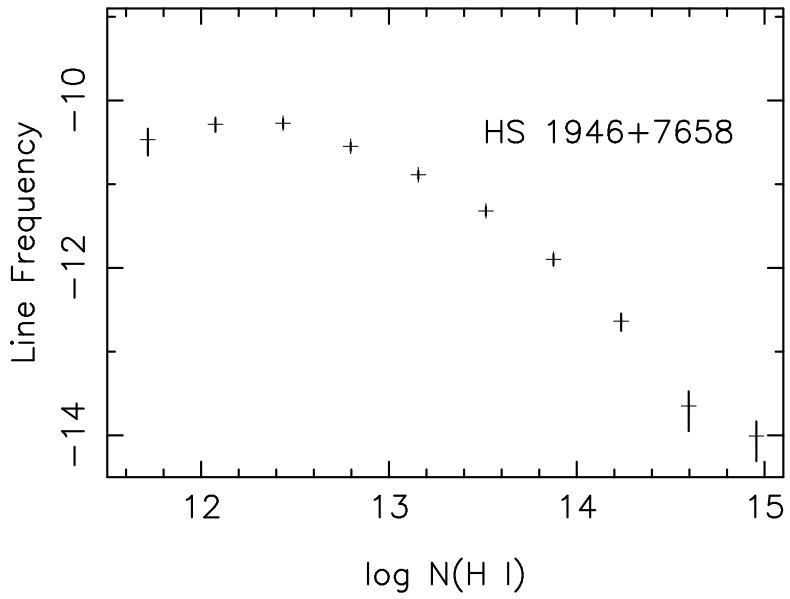

FIG. 3.—Observed N(H I) distribution toward HS 1946+7658. The lines have been binned into intervals of 0.36 in Log N(H I), starting from 11.75. The vertical bars represent 1 σ errors. The first bin has eight lines.

- ◦ Define: $f(N_{\rm HI}, z)dNdz$ is the number of lines with $N_{\rm HI}$ in the interval $(N_{\rm HI}, N_{\rm HI} + dN_{\rm HI})$ and within the redshift interval $(z, z + dz)$
- ◦ Kirkman & Tytler 1997 ($z = 2.7$)
- ◦ Fitting a power-law for $10^{14.} > N_{\rm HI} > 10^{12.1}$

$$f(N, z \approx 2.7) = 6.2 \times 10^8 N_{\rm HI}^{-1.5} \tag{137}$$

◇ Redshift evolution

- ▲ Repeat the analysis at a range of redshift
- ▲ Simply count up lines in the same $N_{\rm HI}$ interval
  - ◦ To confuse us, this is often referred to as dn/dz or dN/dz
  - ◦ I prefer $\ell(z)$, a line density
  - ◦ Power-law fit (Lu et al. 1991)

$$\ell(z) = A(1+z)^{\gamma} \tag{138}$$
$$= 2.67(1+z)^{2.37\pm0.26} \tag{139}$$

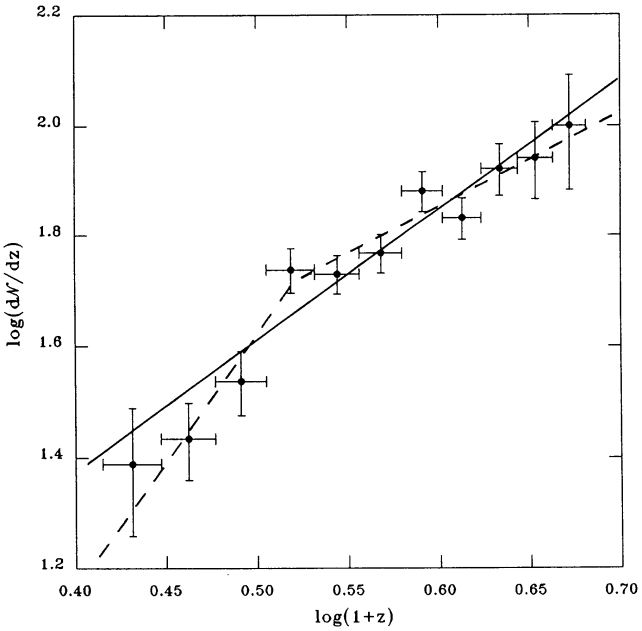

FIG. 1.—log ($d\mathcal{N}/dz$) plotted as a function of log (1 + z) for the full sample. The data are binned solely for the purpose of illustration; the vertical bars are the 1 σ errors, and the horizontal bars represent the chosen ranges of redshift intervals. The solid line is the fit with the single power law (eq. [5] with $\gamma = 2.37$, $A = 2.67$), and the dashed curve is the fit with the broken power law (eqs. [23]–[24]).

- Cosmology
  - ◇ Interpret Lyα 'clouds' as large-scale (Mpc) density ripples
    - ▲ Fluctuating Gunn-Peterson
    - ▲ This picture, inspired by numerical simulations, beget the "Cosmic Web" paradigm (Miralda-Escudé et al. 1996)
  - ◇ Lyα clouds arise at mild overdensities in the universe $\rho \sim$ few ρ_c

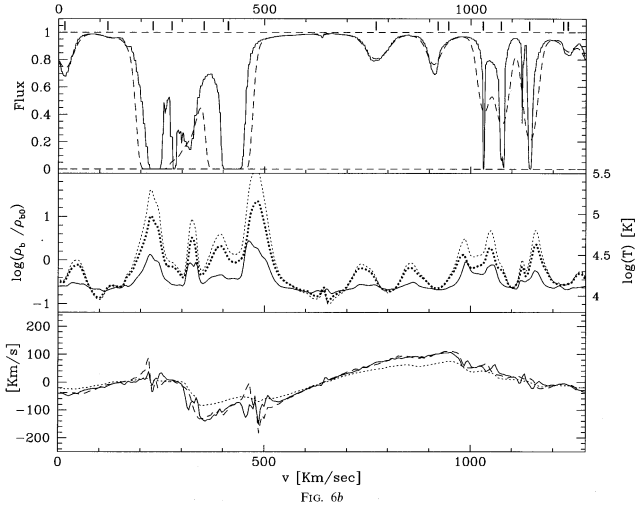

FIG. 6b

FIG. 6.—Middle panel in each figure shows the gas density along a row, in units of the average gas density (*thick dotted line*; *left vertical axis*), the gas temperature (*solid line*; *right vertical axis*), and the gas pressure (*thin dotted line*; the same scale as density but arbitrary units). Spatial coordinate in horizontal axis is $x = v/H$. Rows shown in (*a*), (*b*), (*c*), and (*d*) are marked as dashed lines in slice in Fig. 5. Calculated Lyα absorption spectrum is in top panel, without thermal broadening (*solid line*), and including it (*dashed line*). Tickmarks in upper part of top panel indicate the position of fitted lines in Table 2. Peculiar velocity is shown as dotted line in bottom panel, together with gravitational acceleration (*dashed line*) and total acceleration (*solid line*) divided by the Hubble constant.

◇ This picture gives a good match to the key observables

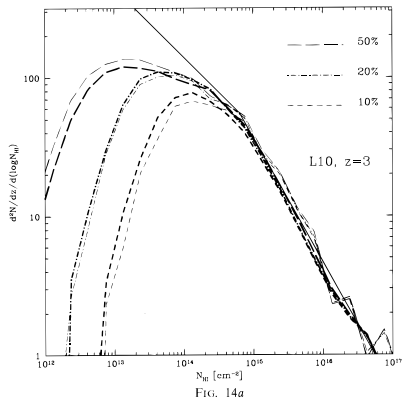

FIG. 14a

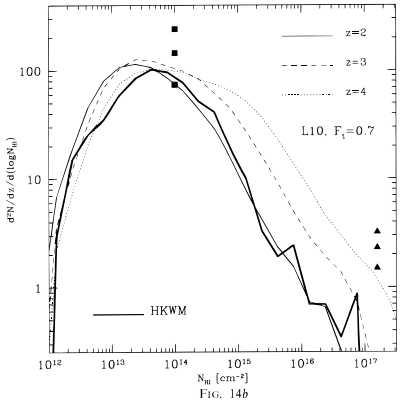

FIG. 14b

FIG. 14.—(*a*) Thick lines are column density distribution at $z = 3$ in the L10 simulation for filling factors 10%, 20%, and 50% (corresponding to flux thresholds $F_t = 0.107$ 0.486, and 0.891, respectively). Results for line model are shown as thin lines, thin solid line is the true column density distribution of line model. (*b*) Column density distribution for flux threshold $F_t = 0.7$, at $z = 2$, 3, and 4. Black squares are observed number of lines at $N_{\rm H\,I} = 10^{14}$ cm^{-2} at $z = 3$ from Petitjean et al. (1993), and assuming evolution as $(1 + z)^{2.3}$ for $z = 2$ and $z = 4$. Black triangles are number of Lyman limit systems at $z = 2$, 3, and 4 from Stengler-Larrea et al. (1995; we assume a slope $\beta = 1.5$ of the column density distribution to transform their cumulative number of Lyman limit systems to a differential number). The thick solid line is the distribution obtained by HKWM (using an SPH simulation and for a CDM model different from the one we adopt).

▲ But, the results have little sensibity to cosmological parameters

▲ The key quantity that matters is the ratio of the baryon density to the ionization rate Γ via the EUVB

$$\mu \propto \frac{\Omega_b^2 h^3}{\Gamma} \tag{140}$$

◇ Redshift evolution is primarily a consequence of $n \propto (1 + z)^3$

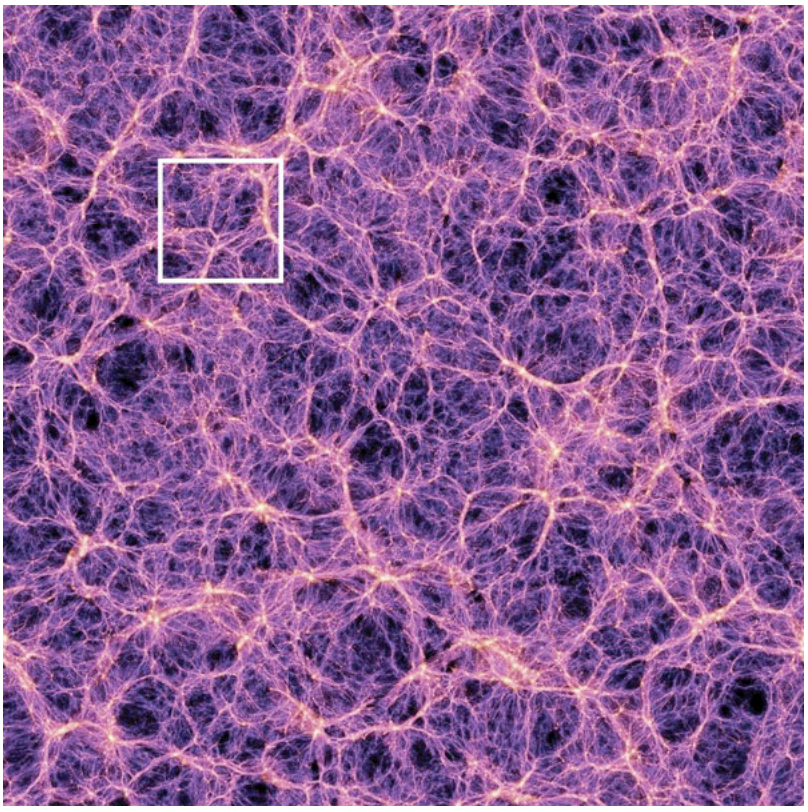

- Modern techniques
  - ◇ Avoid counting lines (arbitrary and time consuming)
  - ◇ Characterize the full effect of the Lyα forest as an effective opacity
    - ▲ Measured over an ensemble (i.e. large number) of quasars
    - ▲ Envisiong averaging 100 quasar spectra

$$\tau_{eff}(z) = -\ln\left[\frac{I_\nu}{I_\nu^*}\right] \tag{141}$$

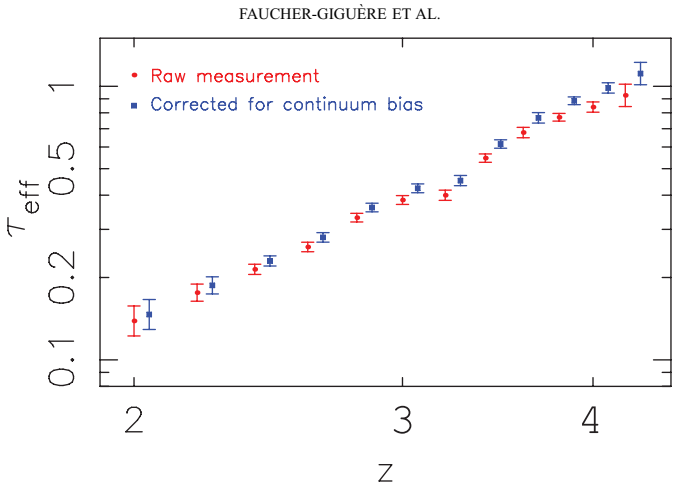

  - ◇ Compare these measurements against numerical simulations